Resonances via deterministic and stochastic perturbations: A comparative study

Gerardo J. Escalera Santos and P. Parmananda
Facultad de Ciencias, UAEM, Avenida Universidad 1001, Colonia Chamilpa, Cuernavaca, Morelos, Mexico
(Received 16 November 2001; published 19 June 2002)

We study periodic and coherence resonances invoked by aperiodic yet deterministic perturbations. Chaotic perturbations with varying levels of intrinsic correlations are superimposed parametrically on an excitable chemical model. This enables us to analyze the system response and characterize the induced resonances as a function of correlation in the perturbing signal. Using standard measures such as normalized variance and normalized number of peaks, dynamics for different deterministic signals are quantified and eventually compared to resonances invoked via stochastic perturbations.

DOI: 10.1103/PhysRevE.65.067203 PACS number(s): 05.45.−a

I. INTRODUCTION

Stochastic resonance (SR) [1] is a term used to define a process in which addition of a random (noise) function to a preexisting subthresold deterministic signal, results in the amplification of the deterministic signal. An optimum amplification (intensity and fidelity) of the previously weak deterministic signal is achieved for a particular level of superimposed noise intensity. Subsequent to an initial latency period, this field has attracted a lot of attention, and SR has been detected and analyzed [2,3] in a number of physical [4], chemical [5], and biological [6] systems. More recently, another related resonance effect has been investigated [7]. Coherence resonance (CR) records the inception of maximum coherence in noise excited oscillations for an optimum noise amplitude [7]. It is observed in noise driven excitable systems, where an interplay between statistical properties of excitatory and refractory periods [7] with external noise results in the emergence of coherence (regularity). The two resonance effects are different as in CR, there is no external deterministic signal being enhanced by virtue of superimposed noise.

All of these previously mentioned results involving stochastic and coherence resonances used white noise with a Gaussian distribution as the perturbing function. However, there exists some works in the existing literature that study the resonance invoked via deterministic perturbations [8–10]. Specifically, the work of Carroll and Pecora [8,9] using chaotic signals was motivated by the fact that resonances induced by deterministic signals could perhaps be understood using the concepts of nonlinear dynamics and bifurcation theory. In this paper, we study both periodic and coherence resonances using chaotic perturbations with different correlations. Using standard measures (normalized variance and number of peaks), we compare the induced deterministic resonances, eventually comparing them with resonances invoked via a stochastic perturbation (Gaussian white noise). The paper is organized as follows: The excitable chemical system used to study the different resonances is presented in the following section. Coherence resonances induced via deterministic (aperiodic) and stochastic perturbations are compared in Sec. III. Periodic resonances invoked by deterministic and stochastic perturbations are compared in Sec. IV. Finally, a brief discussion of the obtained results is presented in Sec. V.

II. NUMERICAL MODEL

The model system under consideration involves passivation of the reactive surface of a metal electrode in an electrochemical cell. The chemical kinetics of the passivation model include formation of a surface film, MOH, where M represents the metal atom [11]. The chemical kinetics lead to the following dimensionless equations [12]:

$$\dot{Y} = p(1-\theta_{\mathrm{OH}}) - qY, \tag{1}$$

$$\dot{\theta}_{\mathrm{OH}} = Y(1-\theta_{\mathrm{OH}}) - [\exp(-\beta\theta_{\mathrm{OH}})]\theta_{\mathrm{OH}}, \tag{2}$$

where Y is the concentration of metal ions in the electrolyte, and θ_{OH} is fraction of the metal surface covered by metal hydroxide. The system parameters p and q are related to chemical rate constants, and β represents the non-Langmuir nature of MOH film formation. The system has been studied in some detail [12] and is oscillatory subsequent to a Hopf bifurcation for the parameter values $(p,q,\beta) = (1.327\,76 \times 10^{-4}, 1.0\times 10^{-3}, 5.0)$. Designating this bifurcation point as the parameter threshold, we choose $p_0 < 1.327\,76 \times 10^{-4}$, such that the system exhibits steady state dynamics. Subsequently, external perturbations are parametrically superimposed on the system parameter p, enabling us to analyze the invoked resonances.

III. INVOKED COHERENCE RESONANCE

The set point of the autonomous model system ($p_0 < 1.327\,76\times 10^{-4}$) is such that the dynamical response is a stable fixed point. Aperiodic perturbations are generated from the time series of Lorenz attractor [13]. By choosing successively larger sampling intervals, perturbations with worsening correlations can be generated. For example, starting from the chaotic time series of the Lorenz attractor, if one samples every hundredth point of the original time series, a time series with a weaker correlation (than the original) would be generated. Continuing with this strategy, intrinsic correlation of the perturbing signal can be systematically varied. The system parameter p is continuously varied in the following manner,

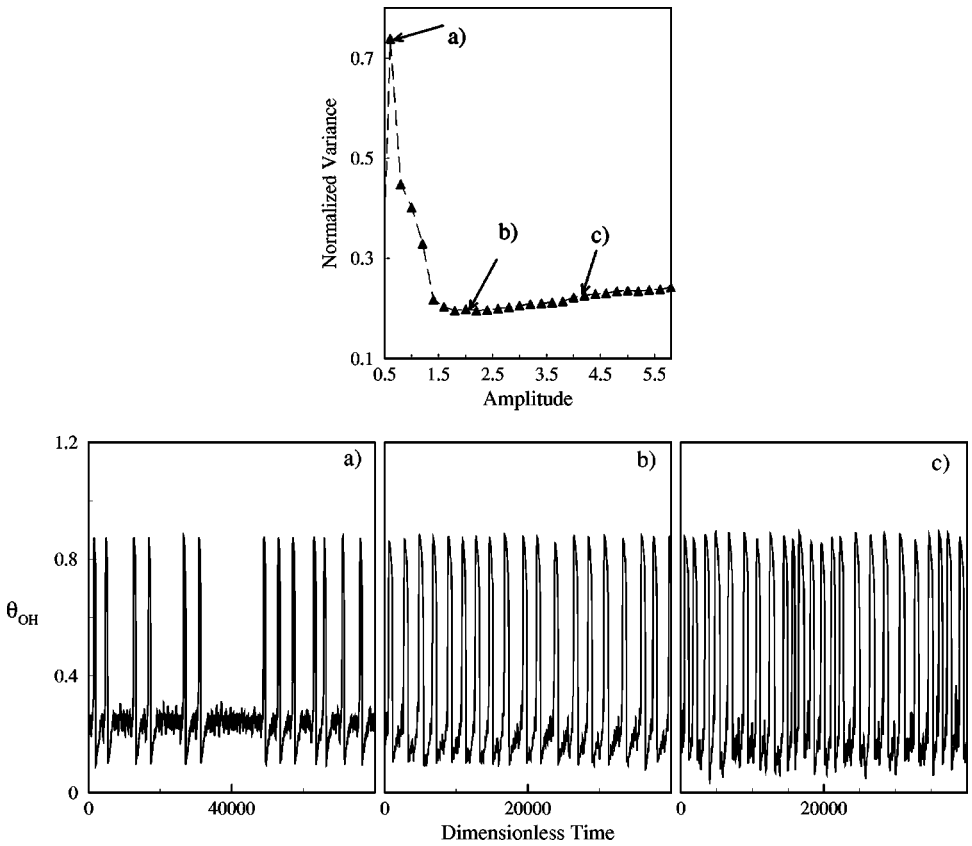

FIG. 1. The normalized variance curve computed for a chaotic Lorenz time series with a time delay of 0.1 (dimensionless model time). The maximum periodicity induced corresponds to the minima of the resonance curve. Time series observed for three different amplitudes of the superimposed perturbation [demarcated (a), (b), (c) in the calculated curve] are shown in the lower part of the figure.

$$p = p_0(1 + \delta p), \tag{3}$$

where δp is the aperiodic time series of the Lorenz attractor, generated as explained above.

The dynamical response of the model to the superimposed perturbations varying in amplitude and correlations is quantified using normalized variance (V_N) [7]. It is defined as

$$V_N = \frac{\sqrt{\mathrm{var}(t_p)}}{\langle t_p \rangle}, \tag{4}$$

where t_p is the time between successive peaks. The upper part of Fig. 1, shows the calculated V_N [7] as a function of the amplitude of perturbing signal. The V_N function is a U-shape curve, where the minima corresponds to the maximal coherence induced. The lower part of Fig. 1, shows the time series of a system variable θ_{OH} invoked by superimposed perturbations. The three profiles presented correspond to the three points demarcated on the U-shaped normalized variance curve. It indicates that for an optimum value of perturbation amplitude, regular spiking is induced via aperiodic perturbations. Figure 2 shows the resonance curves computed for deterministic perturbations with varying correlations. Also plotted is the coherence resonance curve induced by stochastic perturbations. It is observed, as expected, that the curves obtained for deterministic perturbations with weaker correlations tend to the one generated via stochastic perturbation. It is also evident from Fig. 2, that deeper minimas in the coherence resonance curves are observed for deterministic perturbations with stronger correlations. It implies that, more regular spike trains can be invoked for perturbations with stronger intrinsic correlations. Finally, optimum value of the perturbation amplitude at which maximal coherence is observed (minima of the resonance curve), is larger for perturbations with stronger correlations. To summarize, it is possible to observe coherence resonance for deterministic perturbations. Moreover, calcu-

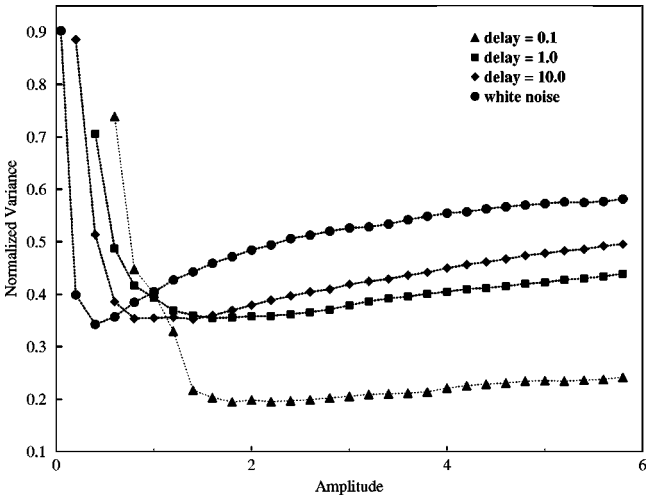

FIG. 2. Various coherence curves computed for deterministic and stochastic perturbations. Figure legends indicate the different delay times (dimensionless model units) used to generate deterministic perturbations with varying correlations.

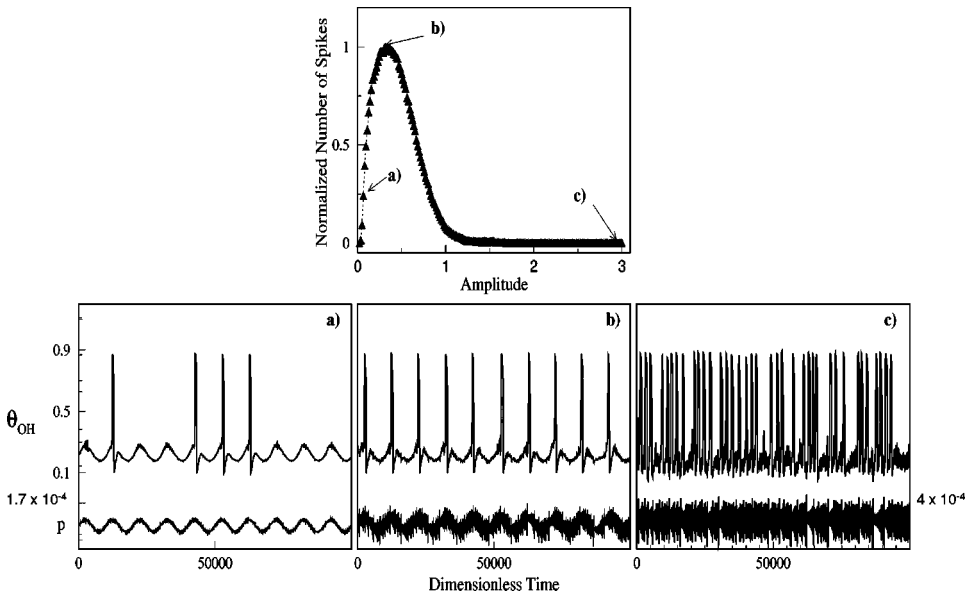

FIG. 3. The normalized number of spikes curve computed for a chaotic Lorenz time series with a time delay of 0.1 (dimensionless model time). The maximum periodicity induced corresponds to the maxima of the resonance curve. Time series observed for three different amplitudes of the superimposed perturbation [demarcated (a), (b), (c) in the calculated curve] are shown in the lower part of the figure. Also presented in this figure is the superimposed perturbation, a composite of the subthreshold sinusoidal signal and the chaotic fluctuations.

lated resonance curves for low-correlation deterministic signals and stochastic perturbations tend to converge.

IV. INVOKED PERIODIC RESONANCE

Similar to the case of coherence resonance, the model is placed at ($p_0 < 1.327\,76 \times 10^{-4}$), such that the dynamical response is a stable fixed point. The system parameter p is continuously varied

$$p = p_0[1 + a\,\sin(\omega t) + \delta p], \tag{5}$$

where $a\,\sin(\omega t)$ is the subthreshold periodic signal such that $p_0(1+a) < 1.327\,76 \times 10^{-4}$ and δp are the aperiodic perturbations generated from the time series of Lorenz attractor [13]. Intrinsic correlation of the perturbing function are varied using the recipe described in the preceding section.

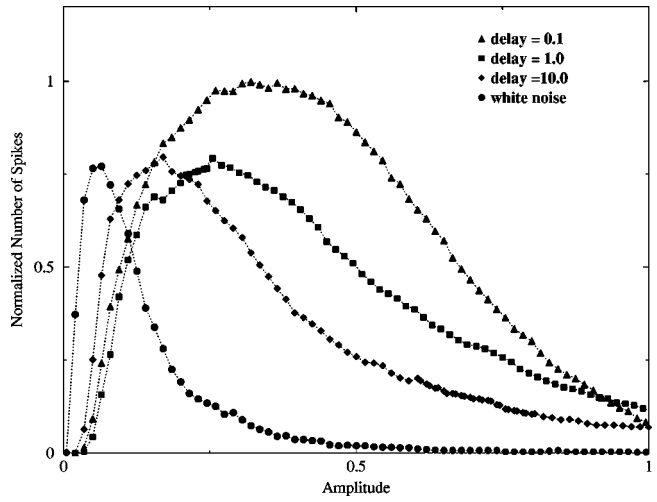

FIG. 4. Various periodic resonance curves computed for deterministic (with varying correlations) and stochastic perturbations. Figure legends indicate the different delay times (dimensionless model units) used to generate deterministic perturbations with varying correlations.

The induced responses are quantified using normalized number of spikes (NNS) [14,15]. The upper part of Fig. 3, shows a typical resonance curve obtained, plotting NNS, a function of the amplitude of the deterministic perturbation. The maxima of the curve represents the optimum amplification of the subthreshold periodic signal for a particular amplitude of the aperiodic signal. Three representative time series (corresponding to three points demarcated in the resonance curve) of the invoked system dynamics are shown in the lower graphs. Also superimposed is the subthreshold sinusoidal signal. The optimal amplification of the subthreshold signal is evident for the time series in the middle [corresponding to the point (b) of the resonance curve]. Figure 4 shows different resonance curves computed for varying intrinsic correlations. Also shown are the results obtained for white noise [14,15]. Similar to the results of the preceding section, resonance curves for deterministic signals with weak correlations approach the curve for stochastic perturbations. Moreover, as expected, maxima of the resonance curve is higher for signals with stronger correlations.

V. DISCUSSION

As indicated by our results, resonance phenomena observed in the presence of stochastic perturbations can also emerge for deterministic perturbations. This is consistent with the results of Carroll and Pecora [8,9]. Using standard measures such as normalized variance and normalized number of spikes, we were able to compare and contrast resonances observed for stochastic and deterministic perturbations (with varying level of intrinsic correlations). We propose using different sampling intervals as an efficient way of varying the correlation of the superimposed signal. Signals with varying correlations invoke distinct system responses as manifested by the shifts in the induced resonance curves.

ACKNOWLEDGMENT

This work has been supported by CONACyT, Mexico.

[1] R. Benzi, A. Sutera, and A. Vulpiani, J. Phys. A **14**, 453 (1981).
[2] P. Jung, and G. Mayer-Kress, Phys. Rev. Lett. **74**, 2130 (1995).
[3] P. Jung and G. Mayer-Kress, Chaos **5**, 458 (1995).
[4] F. Moss, A. Bulsara, and M.F. Shlesinger, J. Stat. Phys. **70**, 1 (1993).
[5] A. Guderian, G. Dechert, K.P. Zeyer, and F.W. Schneider, J. Phys. Chem. **100**, 4437 (1996).
[6] F. Moss, D. Pierson, and D. O'Gorman, Int. J. Bifurcation Chaos Appl. Sci. Eng. **4**, 1383 (1994).
[7] Arkady S. Pikovsky and Jürgen Kurths, Phys. Rev. Lett. **78**, 775 (1997).
[8] T.L Carroll and L.M. Pecora, Phys. Rev. Lett. **70**, 576 (1993).
[9] T.L Carroll and L.M. Pecora, Phys. Rev. E **47**, 3941 (1993).
[10] Tsuyoshi Hondou and Yasuji Sawada, Phys. Rev. E **54**, 3149 (1996).
[11] J.B. Talbot and R.A. Oriani, Electrochim. Acta **30**, 1277 (1985).
[12] J.K. McCoy, Punit Parmananda, R.W. Rollins, and Alan J. Markworth, J. Mater. Res., **8**, 1858 (1993).
[13] E.N. Lorenz, J. Atmos. Sci. **20**, 130 (1963).
[14] W. Hohman, J. Müller, and F.W. Schneider, J. Phys. Chem. **100**, 5388 (1996).
[15] Takashi Amemiya, Takao Ohmori, Masarau Nakaiwa, and Tomohiko Yamaguchi, J. Phys. Chem. A **102**, 4537 (1998).